NORSAR ROYAL NORWEGIAN COUNCIL FOR SCIENTIFIC AND INDUSTRIAL RESEARCH

NORSAR Scientific Report No. 1-86/87

SEMIANNUAL TECHNICAL SUMMARY

1 April - 30 September 1986

L.B. Loughran (ed.)

Kjeller, November 1986

VII.4 Optimum beam deployment for NORESS P-wave detection

In order to realistically assess the potential of the NORESS array for event detection, it is necessary to compute the actual beamforming gain for a variety of representative seismic signals. In previous investigations (Mykkeltveit et al, 1985; Fyen, 1986) we focussed on the noise suppression obtained for various NORESS subgeometries. This contribution deals with the signal loss (by beamforming) in addition to the noise suppression, and the two quantities are combined to obtain the beamforming gain.

The main objective of this study is the recommendation of an optimum set of beams for the detection of regional and teleseismic P-waves at NORESS. This requires that for each frequency band we must find the subgeometry that gives the best beamforming gain. For each frequency band it is also necessary to determine whether one single vertical (infinite velocity) beam is adequate. Alternatively, steered beams with delays corresponding to several slownesses and azimuths are needed. Because of the potential for reduction in computation time, it is important to identify the classes of signals for which vertical beams will do.

Analysis method

Under the condition of approximately equal signal and noise amplitudes at each sensor, we can express the beamforming gain G by the normalized zero-lag cross-correlations via the formula:

$$G^2 = \sum_{i,j=1}^{N} w_i w_j c_{ij} \Big/ \sum_{i,j=1}^{N} w_i w_j \rho_{ij} \qquad (1)$$

where c_{ij} is the signal correlation between sensors i and j and ρ_{ij} is the corresponding noise correlation. N is the number of sensors used and w_i are sensor weights. The signal loss and noise suppression are related to the numerator and denominator, respectively, of the above fraction:

$$\text{Signal loss} = \left[\sum_{i,j=1}^{N} w_i w_j \Big/ \sum_{i,j=1}^{N} w_i w_j c_{ij} \right]^{\frac{1}{2}}$$

$$\text{Noise suppression} = \left[\sum_{i,j=1}^{N} w_i w_j \Big/ \sum_{i,j=1}^{N} w_i w_j \rho_{ij} \right]^{\frac{1}{2}}$$

and hence

Gain = Noise suppression / Signal loss

We are now faced with the task of computing the beamforming gain for a variety of different weighting schemes for each signal in our data base. The investigation is restricted to the seven frequency bands 1.0-3.0 Hz, 1.5-3.5 Hz, 2.0-4.0 Hz, 2.5-4.5 Hz, 3.0-5.0 Hz, 4.0-8.0 Hz and 8.0-16.0 Hz. These are the frequency bands currently utilized in the detection processing part of the NORESS online processor (RONAPP). The gain is computed for all possible weighting schemes for which all elements of each ring of the NORESS geometry (see Fig. VII.4.1) have either weight 1 or weight 0. The central element A0 counts as a 'ring' in this regard. We are thus restricitng our search to symmetrical sub-geometries, which ensure equal detection capability in all directions. With five rings in the NORESS geometry there are 31 different sub-geometries, for which the gain is computed. For a given frequency, it is a priori obvious that certain geometries will be clearly inferior to others. Nevertheless, we compute the gain for the whole range of geometries for all frequency bands, because of consistency and because the complete results give useful insight with respect to the properties of signals and noise.

For each of the seven partly overlapping frequency bands, we have selected up to four high SNR regional and/or teleseismic P-wave signals. We have chosen events with peak signal frequencies close to the lower cutoff of that band. This is done in order to ensure that the signal is analyzed in the band for which the SNR for that signal attains its maximum value. The approach chosen will satisfy this requirement since the noise amplitudes are monotonically decreasing with increasing frequencies in the range 1.0-16.0 Hz.

Results

The gains are computed both for a vertical beam and for a beam steered to the broadband slowness vector of the signal (for details on the broadband frequency-wavenumber algorithm used, see section VII.1 of this Semiannual Technical Summary). Before computing the gains for the steered beams, the signals are resampled at 200 Hz (the sampling rate for NORESS data is 40 Hz). The signal loss is computed for a 1-second data window at the signal peak and within 3 seconds from the arrival onset time. The data window length of 1 second is chosen to match the STA window length of the online detector. The noise suppression estimates are based upon 100 seconds of noise ahead of the signal, and are made for the appropriate beams. Finally, we estimate the mean noise suppression for four beams, each with an apparent velocity of 8.0 km/s and steered to azimuths of 0, 90, 180 and 270 degrees. In the following, we give results in terms of beamforming gains for each of the seven frequency bands.

1.0-3.0 Hz

Results for one event are given in Table VII.4.1. For each beam type (infinite velocity or steered), the gain, signal loss (Sloss) and noise suppression (Nsupp) are computed for all possible weighting schemes as detailed above. The best gain obtained and the corresponding weighting scheme are given in the first row of each table within Table VII.4.1. The remaining eight configurations below the top row remain fixed for all tables. All gains, etc., are given in decibels. Nsupp8 is the mean noise suppression for the four 8 km/s beams. A0wgt, Arwgt a.s.o. denote the weights applied to A0, the A ring a.s.o.

It is seen from Table VII.4.1 that the steered beams are at best only marginally better than the infinite velocity beams, and the overall best result is in fact obtained for an infinite velocity beam. Results for the other events with peak signal frequencies slightly above 1.0 Hz show that the infinite velocity beam signal losses are generall modest and less than 1 dB for all weighting schemes considered, so the gain is really controlled by the noise suppression that can be achieved. The beam including A0 and the sensors of the C and D rings (altogether 17 sensors) gives the best overall performance, with a gain typically 4 dB above what is obtained using all 25 sensors of the array. So the recommendation is for an infinite velocity beam for this subgeometry, to cover teleseismic signals with peak signal frequencies between 1.0 and 1.5 Hz satisfactorily.

For this frequency band we also show in the bottom part of Table VII.4.1 gains obtained after having extended our weighting scheme. Here, we have allowed weights 0., 0.5 and 1.0 for each ring and computed the gain for all 242 combinations. We see from the table that a very marginal gain improvement is obtained by this extension of the weighting scheme. From these results it is seen that giving weight 0.5 to A0 is better than both omitting A0 and giving it a weight of 1.0. Still, our general finding after checking all frequency bands is that weights different from 0 and 1 at the very best contribute 1.0 dB over the 0/1 weighting scheme, and the best results are obtained for weighting schemes that vary strongly from event to event. Due to these variations, it is found not to be possible to generalize these results, and in the following we confine our discussion and results to the 0/1 weighting scheme.

1.5-3.5 Hz

The geometry including A0, the C and D rings again gives the best gain for nearly all runs (there is one event for which the gain is improved for the steered beam by omitting A0 from the above geometry). Signal losses for the infinite velocity beams are slightly larger than for the 1.0-3.0 Hz band, and steered beams give from 0.5 to 1.2 dB gain improvement relative to the infinite velocity beams. This is a fairly modest improvement, so again the recommendation is for an infinite velocity beam including A0, the C and D rings, basically to capture the signals with peak frequencies in the range 1.5 to 2.0 Hz, the majority of which will be teleseismic.

2.0-4.0 Hz

In order to recommend a beam deployment for this frequency band, one must deal with the question of where low SNR events with peak signal frequencies in the range 2.0 to 2.5 Hz originate. There are certainly many teleseismic events of this kind, and the results are that these will be adequately covered by an infinite velocity beam using again the central element (A0) and the sensors of the C and D rings. For regional events, however, the signal losses are now becoming appreciable for the vertical beams, and one must consider steered beams for such signals. Again, it is the same subgeometry that gives the best gains, and the recommendation is for a number of beams of apparent velocity 8.0 km/s, and with azimuths to cover the circle adequately, either by an even spacing, or by pointing to source regions of particular interest.

2.5-4.5 Hz

We now observe a tendency that the B ring is becoming all more important for the gain, whereas the D ring is of lesser importance. We see from Table VII.4.2 that the signal losses for the infinite velocity beams are considerable for all geometries including the D ring, while on the other hand, the noise suppression is not much improved through inclusion of the D ring. The best single infinite velocity beam includes A0, the B and C rings. The results indicate that for both regional and teleseismic signals the gain can be further improved by up to 4 dB for optimally steered beams. The best configuration for steered beams appears to be A0, the B, C and D rings.

3.0-5.0 Hz

The geometry consisting of A0, the B and C rings is the best one for all tests in this frequency band, irrespective of beams being vertical or steered. For regional and teleseismic events, the gain can be improved by up to 2-3 dB in going to steered beams. The recommendation is then to deploy one infinite velocity beam for the teleseismic events including the 13 sensors of A0, the B and C rings and in addition, a number of pointed beams, including the same 13 sensors, and shifts corresponding to 8 km/s, to adequately cover regional events.

4.0-8.0 Hz

The events analyzed for this frequency band demonstrate that there is no longer one particular subgeometry with a superior performance, as was found for all frequency bands hitherto considered. This is clearly demonstrated by Table VII.4.3, where it is seen that 4 to 5 different geometries give gains that are within 1.5 dB of the highest gain achieved, both for the infinite velocity beams and for the steered beams.

Among signals with peak frequencies in the lower part of this band, we find events at far regional and short teleseismic ranges. One would like to select one infinite velocity beam for detection of these events, but it is not evident which one should be chosen. For local and regional signals in the entire passband 4.0-8.0 Hz, it seems appropriate to choose the geometry A0, B ring and C ring and deploy 8 steered beams of velocity 8 km/s evenly distributed around the circle. The beam pattern of this geometry suggests that 8 beams are sufficient for adequate coverage. Our results indicate that gains of the order of 10 dB could be realistically expected. In consistency with these beams, the one vertical beam could be formed using the same sensors.

The column labelled 'Nsupp8' in the tables is included to indicate what noise suppressions should be expected when typical regional beams of velocity 8 km/s are formed. From the three tables given, it is seen that this noise suppression almost matches the one obtained for vertical beams, with some exceptions for results given for the 2.5-4.5 Hz band (Table VII.4.2). Taking all events in our data base into consideration, it is found that the noise suppression for the 8 km/s steered beams is generally within 1-2 dB of the corresponding infinite velocity beam noise suppression.

8.0-16.0 Hz

Vertical beams make no sense in this frequency band. The interest in detection in this band is limited to local and regional signals, and the detection beams must be steered to the Pn phase velocity of 8.0 km/s, with a minimum of 8 beams to ensure adequate coverage. A good choice of geometry might be the 8 sensors A0, the A and B rings. A good alternative might be the deployment of one so-called incoherent beam, see below.

Summary and recommendations

The main results of this study are summarized in Figs. VII.4.2 and VII.4.3. Fig. VII.4.2 shows the average beam gains as a function of the lower cutoff frequency of the 7 bands, for 4 selected geometries. This figure comprises both regional and teleseismic events. Fig. VII.4.3 shows, for teleseismic events only, the difference between the gains for steered beams and for the corresponding infinite velocity beams. We see that for 2 Hz and below these differences are very modest but then increase rather abruptly at 2.5 Hz for several of the geometries, indicating the importance of steered beams from this frequency upwards. By combining the two figures, it is seen that vertical beams for at least one of the two subgeometries 1) A0, C and D ring and 2) A0, B and C ring provide more than 10 dB gain for teleseismic events with peak frequencies in the bands with lower cutoff up to and including 3.0 Hz. For higher frequencies steered beams are required in order to achieve 10 dB gain for teleseismic signals.

To achieve similar gains for the regional signals, even more steered beams must be deployed. A viable alternative here is the use of incoherent beams, which are already used by RONAPP for the detection of secondary phases, see Ringdal (1985). The use of a few such beams in the detection of high frequency regional P phases may reduce substantially the number of coherent beams otherwise needed. The recommendations for coherent beam deployment as resulting from this study are summarized in Table VII.4.4.

The results obtained in this study have been compared to SNR gains computed directly in the time domain, with measurements of maximum noise and signal amplitudes. The results confirmed the findings in this investigation.

T. Kværna
S. Mykkeltveit

References

Fyen, J. (1986): NORESS noise spectral studies, preliminary report. Semiannual Technical Summary, 1 October 1985 - 31 March 1986, NORSAR Sci. Rep. No. 2-85/86, Kjeller, Norway.

Mykkeltveit, S., D.B. Harris and T. Kværna (1985): Preliminary evaluation of the event detection and location capability of the small-aperture NORESS array. Semiannual Technical Summary, 1 October 1984 - 31 March 1985, NORSAR Sci. Rep. No. 2-84/85, Kjeller, Norway.

Ringdal, F. (1985): Initial results from NORESS detection processing. Final Technical Report, 1 April - 30 September 1985, NORSAR Sci. Rep. No. 1-85/86, Kjeller, Norway.

1.0-3.0 Hz

Results for infinite velocity beams:

AOwgt	Arwgt	Brwgt	Crwgt	Drwgt	Gain	Sloss	Nsupp	Nsupp8
1	0	0	1	1	13.21	0.35	13.56	12.40
1	1	1	1	1	9.64	0.26	9.90	9.63
1	0	0	0	1	10.56	0.54	11.10	10.46
1	0	0	1	1	13.21	0.35	13.56	12.40
1	0	1	1	1	11.21	0.16	11.37	11.06
1	1	1	1	0	6.16	0.00	6.16	6.02
1	0	1	1	0	7.17	0.00	7.17	6.94
1	1	1	0	0	2.53	0.00	2.53	2.62
1	1	0	0	0	0.89	0.00	0.89	0.92

Results for steered beams:

AOwgt	Arwgt	Brwgt	Crwgt	Drwgt	Gain	Sloss	Nsupp
1	0	0	1	1	12.99	0.00	12.99
1	1	1	1	1	9.77	0.00	9.77
1	0	0	0	1	11.04	0.09	11.13
1	0	0	1	1	12.99	0.00	12.99
1	0	1	1	1	11.21	0.00	11.21
1	1	1	1	0	6.24	0.00	6.24
1	0	1	1	0	7.22	0.00	7.22
1	1	1	0	0	2.63	0.00	2.63
1	1	0	0	0	0.91	0.00	0.91

Results for infinite velocity beams, extended weighting scheme:

AOwgt	Arwgt	Brwgt	Crwgt	Drwgt	Gain	Sloss	Nsupp
0.5	0.0	0.0	1.0	1.0	13.27	0.35	13.62
0.0	0.0	0.0	1.0	1.0	13.15	0.35	13.50
0.5	0.0	0.0	0.5	1.0	13.13	0.37	13.50
1.0	0.0	0.0	0.5	1.0	13.00	0.38	13.38
1.0	0.0	0.5	0.5	1.0	11.99	0.35	12.34

Table VII.4.1 Gain results for one of the events analyzed in this frequency band. The signal had a peak frequency of 1.4 Hz, an SNR (online) of 91.8, apparent velocity 16.37 km/s and arrival azimuth of 14.7 degrees. See the text for explanation of abbreviations.

2.5-4.5 Hz

Results for infinite velocity beams:

AOwgt	Arwgt	Brwgt	Crwgt	Drwgt	Gain	Sloss	Nsupp	Nsupp8
1	0	1	1	0	13.18	1.11	14.29	11.70
1	1	1	1	1	9.67	3.88	13.55	9.63
1	0	0	0	1	-0.55	9.90	9.35	10.17
1	0	0	1	1	7.18	6.02	13.20	13.56
1	0	1	1	1	10.00	4.44	14.44	13.97
1	1	1	1	0	10.79	0.92	11.71	9.62
1	0	1	1	0	13.18	1.11	14.29	11.70
1	1	1	0	0	4.87	0.26	5.13	4.58
1	1	0	0	0	1.36	0.08	1.44	1.31

Results for steered beams:

AOwgt	Arwgt	Brwgt	Crwgt	Drwgt	Gain	Sloss	Nsupp
1	0	1	1	1	13.98	0.54	14.52
1	1	1	1	1	12.78	0.45	13.23
1	0	0	0	1	8.87	1.01	9.89
1	0	0	1	1	13.00	0.63	13.63
1	0	1	1	1	13.98	0.54	14.52
1	1	1	1	0	11.14	0.00	11.14
1	0	1	1	0	13.58	0.00	13.58
1	1	1	0	0	4.72	0.00	4.72
1	1	0	0	0	1.33	0.00	1.33

Table VII.4.2 Gain results for one of the events analyzed in this frequency band. The signal had a peak frequency of 2.6 Hz, an SNR (online) of 238.4, apparent velocity 13.36 km/s and arrival azimuth of 89.1 degrees.

4.0-8.0 Hz

Results for infinite velocity beams:

AOwgt	Arwgt	Brwgt	Crwgt	Drwgt	Gain	Sloss	Nsupp	Nsupp8
1	0	1	0	0	7.69	1.31	9.00	7.96
1	1	1	1	1	3.90	9.90	13.80	13.56
1	0	0	0	1	-4.97	14.89	9.92	10.17
1	0	0	1	1	-5.58	17.72	12.14	12.77
1	0	1	1	1	2.36	12.04	14.40	13.98
1	1	1	1	0	7.23	4.15	11.38	11.06
1	0	1	1	0	7.08	5.04	12.12	12.04
1	1	1	0	0	6.35	1.01	7.36	7.13
1	1	0	0	0	2.32	0.27	2.59	2.73

Results for steered beams:

AOwgt	Arwgt	Brwgt	Crwgt	Drwgt	Gain	Sloss	Nsupp
0	1	1	1	1	12.00	1.94	13.94
1	1	1	1	1	11.49	1.83	13.32
1	0	0	0	1	5.56	4.01	9.57
1	0	0	1	1	9.63	2.62	12.25
1	0	1	1	1	11.97	2.05	14.02
1	1	1	1	0	10.56	0.54	11.10
1	0	1	1	0	11.86	0.54	12.40
1	1	1	0	0	6.41	0.18	6.59
1	1	0	0	0	2.39	0.08	2.47

Table VII.4.3 Gain results for one of the events analyzed in this frequency band. The signal had a peak frequency of 4.6 Hz, an SNR (online) of 264.1, apparent velocity 11.10 km/s and arrival azimuth of 166.3 degrees.

Frequency band Hz	Configuration	Velocity km/s	Azimuths
1.0-3.0	AO C D	∞	
1.5-3.5	AO C D	∞	
2.0-4.0	AO C D	∞	
	AO C D	8.0	(i)
2.5-4.5	AO B C	∞	
	AO B C D	8.0	(i)
3.0-5.0	AO B C	∞	
	AO B C	8.0	(i)
4.0-8.0	several possibilities	∞	
	AO B C	8.0	(ii)
8.0-16.0	AO A B	8.0	(ii)

(i) : These beams could be pointed to source regions of particular interest, or alternatively, distributed evenly around the circle.

(ii) : 8 beams spaced at 45 degrees intervals are recommended.

Table VII.4.4 Recommendation for deployment of coherent beams for optimum detection of P waves on NORESS.

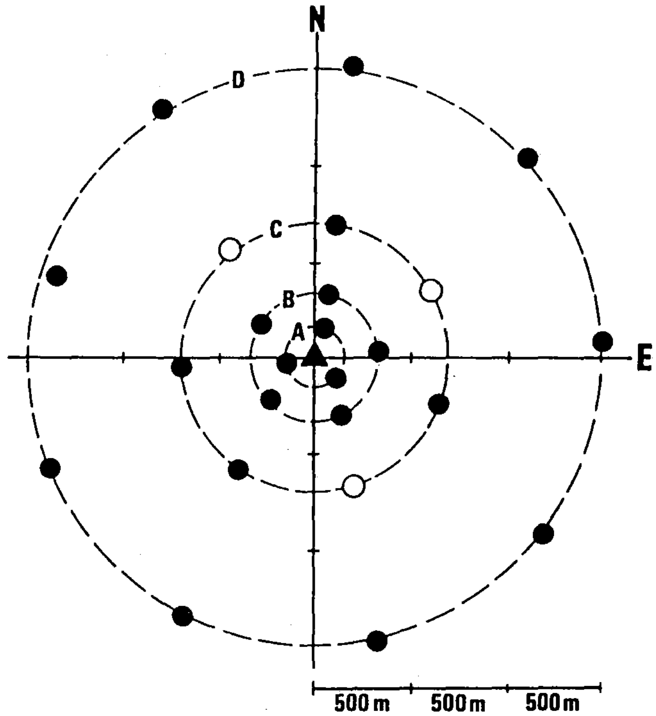

LEGEND:

● VERTICAL SHORT PERIOD

○ 3-COMPONENT SHORT PERIOD

▲ 3-COMPONENT BROAD BAND
AND 3-COMPONENT SHORT PERIOD

Fig. VII.4.1 The geometry of the NORESS array. The instrument at the center is denoted A0. This investigation deals with data from the vertical short period array, comprising one sensor at each of the 25 instrument sites.

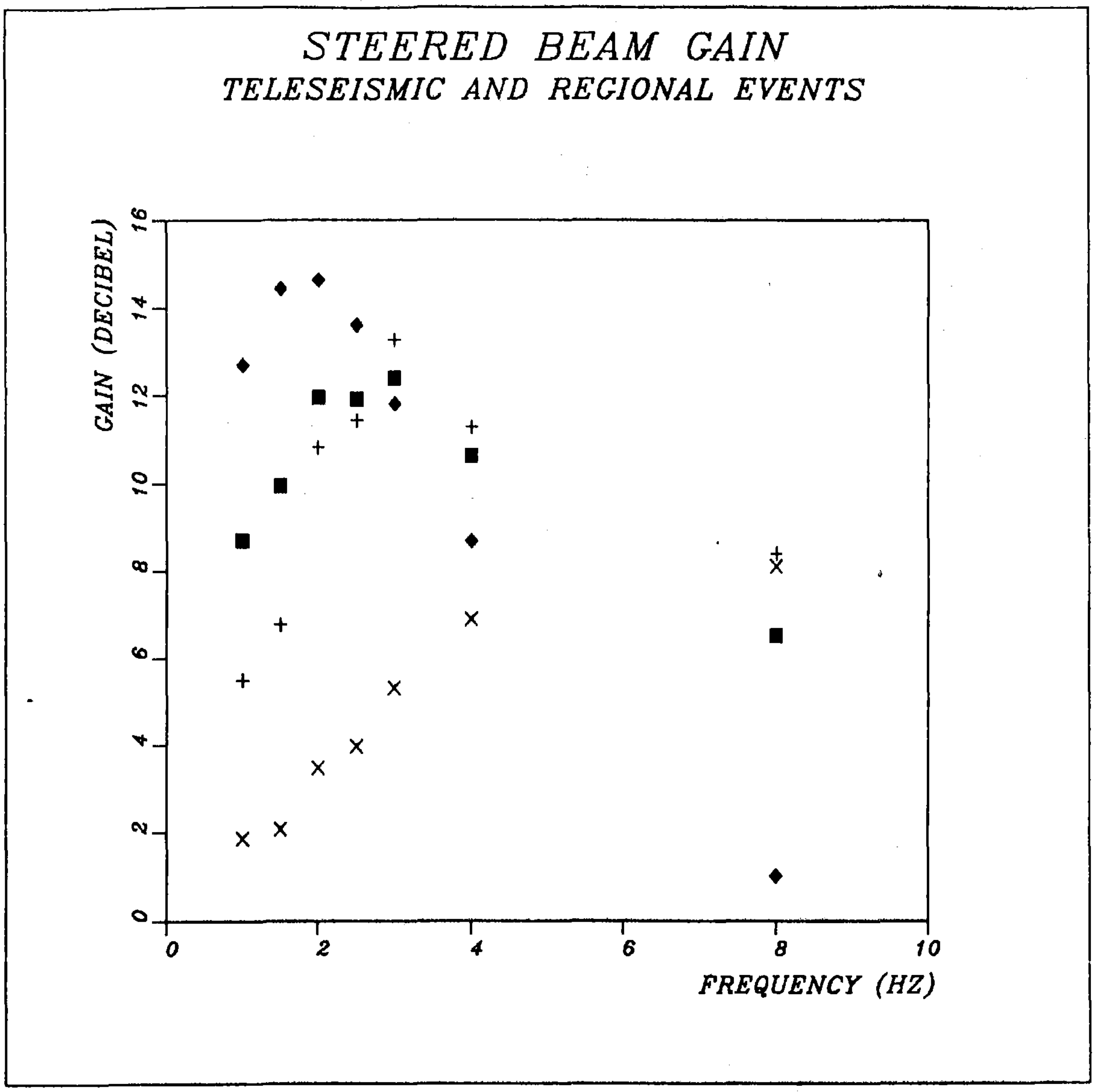

NORESS subgeometries:

◆ A0, C ring, D ring

+ A0, B ring, C ring

■ All sensors

× A0, A ring, B ring

Fig. VII.4.2 Gains for optimally steered beams as a function of lower cutoff frequency for the 7 passbands considered in this study, for 4 selected NORESS subgeometries. For each geometry and frequency, the gain is the average for all events analyzed, both regional and teleseismic.

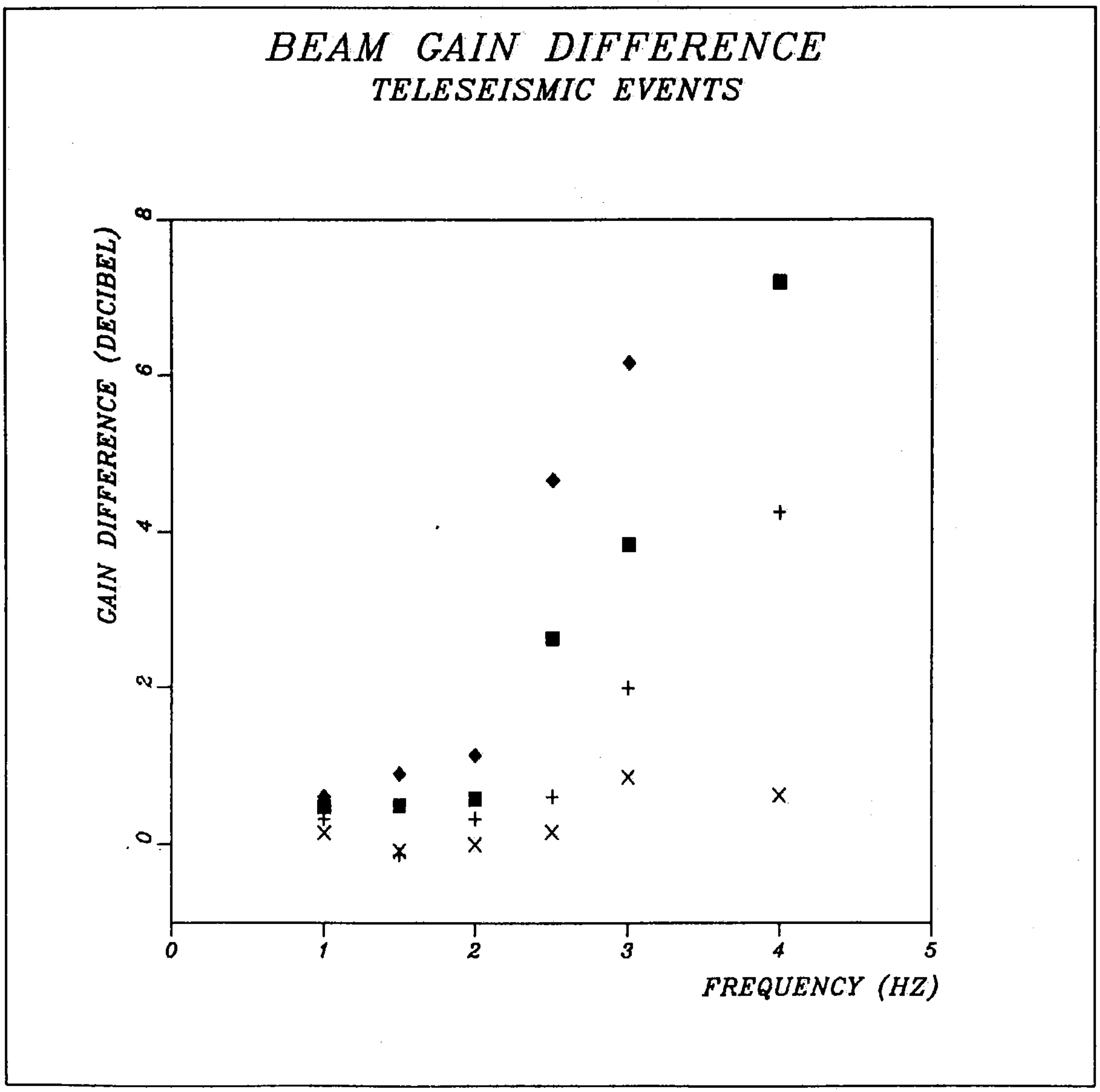

Fig. VII.4.3 The figure shows the differences between the gains for optimally steered beams and for the corresponding vertical beams. Only signals of apparent velocities above 11 km/s have been used. Symbols correspond to the ones in Fig. VII.4.2.